Multimodality Imaging Assessment of Prosthetic Heart Valves

Dominika Suchá, MD, Petr Symersky, MD, PhD; W. Tanis, MD, PhD;
Willem P.Th.M. Mali, MD, PhD; Tim Leiner, MD, PhD; Lex A. van Herwerden, MD, PhD;
Ricardo P.J. Budde, MD, PhD

Abstract—Echocardiography and fluoroscopy are the main techniques for prosthetic heart valve (PHV) evaluation, but because of specific limitations they may not identify the morphological substrate or the extent of PHV pathology. Cardiac computed tomography (CT) and magnetic resonance imaging (MRI) have emerged as new potential imaging modalities for valve prostheses. We present an overview of the possibilities and pitfalls of CT and MRI for PHV assessment based on a systematic literature review of all experimental and patient studies. For this, a comprehensive systematic search was performed in PubMed and Embase on March 24, 2015, containing CT/MRI and PHV synonyms. Our final selection yielded 82 articles on surgical valves. CT allowed adequate assessment of most modern PHVs and complemented echocardiography in detecting the obstruction cause (pannus or thrombus), bioprosthesis calcifications, and endocarditis extent (valve dehiscence and pseudoaneurysms). No clear advantage over echocardiography was found for the detection of vegetations or periprosthetic regurgitation. Whereas MRI metal artifacts may preclude direct prosthesis analysis, MRI provided information on PHV-related flow patterns and velocities. MRI demonstrated abnormal asymmetrical flow patterns in PHV obstruction and allowed prosthetic regurgitation assessment. Hence, CT shows great clinical relevance as a complementary imaging tool for the diagnostic work-up of patients with suspected PHV obstruction and endocarditis. MRI shows potential for functional PHV assessment although more studies are required to provide diagnostic reference values to allow discrimination of normal from pathological conditions. **(*Circ Cardiovasc Imaging*. 2015;8:e003703. DOI: 10.1161/CIRCIMAGING.115.003703.)**

Key Words: computed tomography ■ echocardiography ■ heart valve prosthesis ■ magnetic resonance imaging ■ review, systematic

The number of patients requiring heart valve replacement is increasing rapidly as the population is aging.[1] Monitoring and follow-up of patients with prosthetic heart valves (PHVs) is important because of the numerous and potentially life-threatening complications, such as infective endocarditis, thrombosis, pannus, (peri)prosthetic regurgitation, patient–prosthesis mismatch, and structural failure. The reported incidence of these complications varies from 0.5% to 6% per year[2,3] and depends on prosthesis type, position, and the modalities used for patient monitoring that may impact the diagnostic accuracy. Current imaging modalities include fluoroscopy, which is limited to the assessment of mechanical PHV leaflet motion, and echocardiography.[4] Echocardiography is the mainstay for evaluation of PHV function providing both functional (Doppler) and anatomic information. However, echocardiography may not identify the morphological cause of PHV dysfunction or provide information on its extent because of acoustic shadowing, complex anatomy, and limited viewing windows.[4–6]

Computed tomography (CT) and magnetic resonance imaging (MRI) have established their role in cardiac imaging. Several, yet diverse studies have advocated MRI and more prominently CT as new imaging techniques for PHV assessment to complement echocardiography.[7–15] This review provides a complete, systematic evidence-based literature overview on CT and MRI of PHVs to determine their usefulness as additional imaging modalities for PHV evaluation with an emphasis on imaging feasibility, diagnostic potential, and added value in relation to established techniques.

Literature Review

The search and article were prepared according to the PRISMA statement for reporting systematic reviews and meta-analyses.[16] A comprehensive systematic literature search was performed in

Received June 5, 2015; accepted August 18, 2015.

From the Departments of Radiology (D.S., W.P.Th.M.M., T.L., R.P.J.B.) and Cardiothoracic Surgery (L.A.v.H.), University Medical Center Utrecht, Utrecht, The Netherlands; Department of Cardiothoracic Surgery, VU University Medical Center, Amsterdam, The Netherlands (P.S.); Department of Cardiology, HagaZiekenhuis, The Hague, The Netherlands (W.T.); and Department of Radiology, Erasmus Medical Center, Rotterdam, The Netherlands (R.P.J.B.).

The Data Supplement is available at http://circimaging.ahajournals.org/lookup/suppl/doi:10.1161/CIRCIMAGING.115.003703/-/DC1.

Correspondence to Dominika Suchá, MD, Department of Radiology, University Medical Center Utrecht, Huispostnummer E01.132. Heidelberglaan 100, PO box 85500, 3508 GA Utrecht, The Netherlands. E-mail d.sucha@umcutrecht.nl

PubMed and Embase databases on March 24, 2015, to acquire all studies describing CT/MRI of PHVs, using the algorithm presented in Supplement I in the Data Supplement. In Embase, conference abstracts and articles, letters, notes, and editorials were excluded from the search. No language or other restrictions were imposed. After manual removal of duplicates, articles were selected by screening titles and abstracts based on predefined criteria (Figure 1). The titles and abstracts of selected articles were screened independently by 2 reviewers. Consensus was reached for discordant judgments. Full texts of selected articles were screened, and references of relevant articles and reviews were checked. Articles dealing with homografts or autografts only, experimental CT/MRI systems, simulation studies based on CT/MRI data, duplicate publications and studies without available full text were excluded. Reference and citation check yielded 5 additional articles[17–21] because PHV or CT was not mentioned in title/abstract as defined in the syntax. The selection yielded 136 unique articles including 36 CT and 47 MRI studies on surgical valves and 54 studies on transcatheter prostheses (Figure 1). On the basis of these results, we included only articles on surgical valves for this review. The study characteristics of the included CT and MRI articles are presented in Supplements II and III in the Data Supplement, respectively. Study results were compared with current imaging standards as retrieved from PHV guidelines.

Current Guidelines

Table 1 provides a summarized overview on the current cardiology guidelines for PHV evaluation (American Heart Association/American College of Cardiology,[22] European Society of Cardiology,[23] Zoghbi et al[4]). Transthoracic (TTE) and transesophageal (TEE) echocardiography are the key modalities for both baseline and dysfunction diagnostic work-up. Whereas TTE is readily available and noninvasive, TEE often provides better image quality because of its higher spatial resolution and thus it allows improved detection of PHV-related pathology. The main advantage of echocardiography is that it can provide functional information and baseline postoperative TTE is always available as reference for follow-up purposes. In contrast, detailed anatomic evaluation remains problematic because of acoustic shadowing and PHV metal reverberations. Moreover, operator experience is crucial for proper echocardiographic PHV assessment. The incremental value of fluoroscopy is limited to the assessment of mechanical valve leaflet excursions. As yet, CT is only mentioned briefly in the guidelines as a potential additional imaging tool, whereas MRI is not mentioned at all.

Prosthetic Valves

Numerous surgical PHV types are available and may be separated into 2 main groups: biological and mechanical valves. Mechanical valves include monoleaflet (tilting disk) and bileaflet valves. Biological valves include porcine and pericardial bovine valves (xenografts), which can be stentless, or contain a metal ring or metal struts. Homografts and autografts are human tissue valves and will not be discussed in this review. Mechanical valves require lifelong anticoagulation therapy, whereas biological valves have limited durability because of structural deterioration. The choice of prosthesis type depends on the patients' age, comorbidity, and specific contraindications.[23]

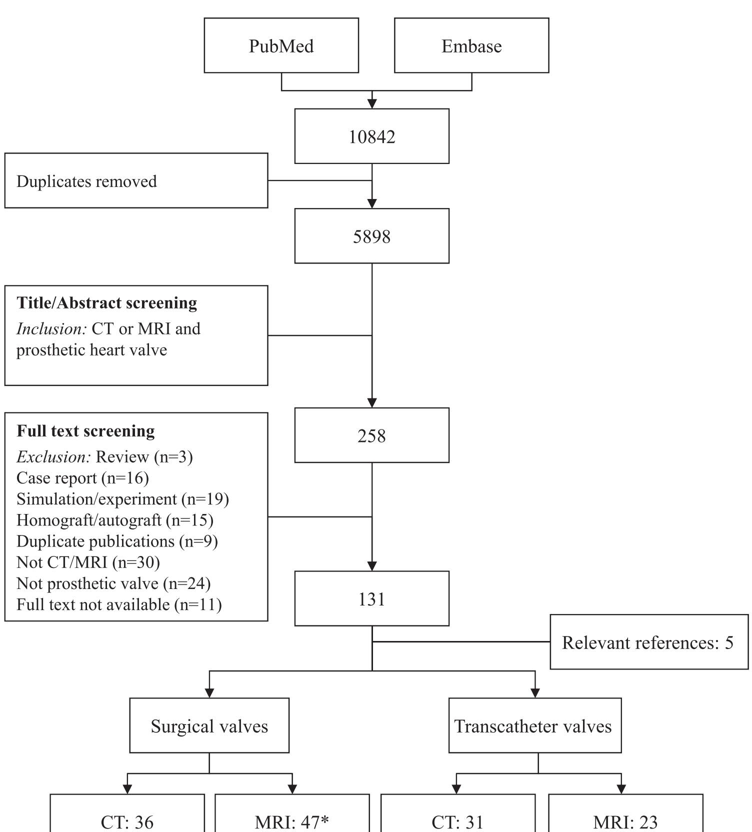

Figure 1. Flowchart of systematic selection of relevant articles *One study included performed both magnetic resonance imaging (MRI) and computed tomographic (CT) imaging

Table 1. Current Guidelines on Prosthetic Heart Valve Evaluation

Indication	Modality	Purpose
Baseline	TTE	6 to 12 wk after implantation, consider before discharge
		Annually after the first 5 to 10 y for bioprostheses or earlier in young patients
Suspected dysfunction	TTE	With new clinical symptoms and/or suspected prosthesis dysfunction
	TEE	Consider if dysfunction suspected
Obstruction	TTE	To assess hemodynamic severity and compare with baseline studies
		To detect patient–prosthesis mismatch
	TEE	To help distinct pannus and thrombus together with clinical parameters
		To assess thrombus size and valve motion
		For close monitoring follow-up of thrombosis
		In nonobstructive valve thrombosis
		After an embolic event
	Fluoroscopy	Only in mechanical valves, to assess valve motion
		For additional information if thrombus/pannus is suspected
	CT	Reasonable: to assess leaflet valve motion
		For additional information if thrombus/pannus is suspected
	Catheterization	If TTE/TEE is insufficient: to assess pressure gradients in aortic valves
Bioprosthesis degeneration	TTE	To detect early structural valve deterioration, leaflet stiffening, calcification, reduced effective orifice area or regurgitation
	TEE	Might be considered: If TTE is inconclusive for imaging biological valve cusps
	CT	Might be considered: If TTE/TEE is inconclusive for imaging biological valve cusps
Regurgitation	TTE	To detect hemodynamic severity of regurgitation
		To detect regurgitation and differentiate valvular from paravalvular regurgitation
	TEE	If TTE is inconclusive to diagnose regurgitation origin, cause and severity
		To detect associated complications
Endocarditis	TTE	To identify vegetations, hemodynamic severity of regurgitation, ventricular function, pulmonary pressures
		To detect endocarditis complications, especially anterior aortic root, such as paravalvular extensions, aneurysms and abscesses
		To re-evaluate known endocarditis with clinical change or high risk-patients
	TEE	In combination with TTE highest diagnostic accuracy for vegetations and perivalvular extension
		If TTE is nondiagnostic or no significant findings but clinical suspicion
		To detect endocarditis complications such as perivalvular abscesses, valve dehiscence and to delineate fistulas and pseudoaneurysms
		Endocarditis if also intracardiac device present
		To re-evaluate known endocarditis with clinical change or high-risk patients
		Intraoperative in endocarditis valve surgery
		Reasonable: for diagnosis in patients with unknown source *S aureus* bacteremia
		Reasonable: for diagnosis in persistent fever without bacteremia or new murmur
		Might be considered: to detect concomitant endocarditis in *S aureus* bacteremia with known extracardiac entry source
	Catheterization	To delineate fistulas and pseudoaneurysms
	CT	Reasonable: to evaluate morphology/anatomy with suspected paraprosthetic infections if echocardiography insufficient for clear anatomic delineation
Valve dehiscence	Fluoroscopy	To detect abnormal tilting or rocking of the base ring (only in extensive dehiscence)
	Catheterization	For diagnosis of small or moderate valve dehiscence

Based on the guidelines of European Society of Cardiology,[23] American Heart Association/American College of Cardiology,[22] and Zoghbi et al.[4] CT indicates computed tomography; and TTE/TEE, transthoracic echocardiography/transesophageal echocardiography.

Computed Tomography

Acquisition

Most studies used retrospective ECG-gated acquisition protocols, which in general are favored over prospective ECG-triggering because they allow cardiac phase reconstructions at 5% to 10% intervals and offer dynamic information on leaflet movement. The radiation dose, however, is relatively high (range [mean], 4±0.5–18.8±3.8 mSv[24,25]). For aortic valves, systolic 20% to 40% and diastolic 70% to 90% reconstructions

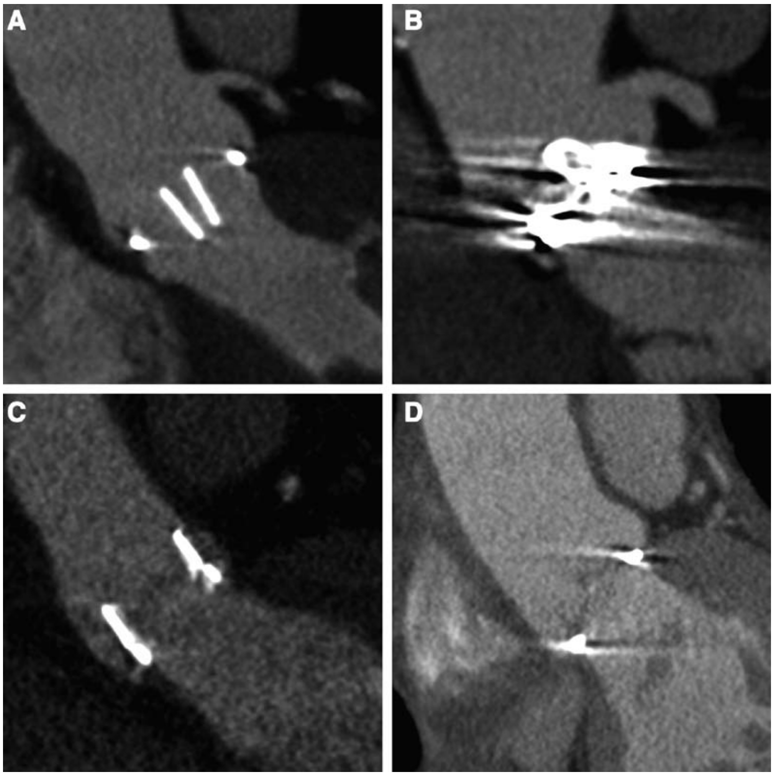

Figure 2. Prosthetic heart valve related artifacts on computed tomography. **A**, St. Jude bileaflet valve, (**B**) Björk-Shiley monoleaflet valve, (**C**) Perimount biological valve, and (**D**) mitroflow biological valve.

usually yield the best images.[25,26] Adjusted double oblique planes provide short-axis views in plane with the prosthesis ring and 2 views parallel and perpendicular to the prosthetic leaflets.[27] Short-acting β-blockers have been administered to reduce patients' heart rate and improve image quality although no article reported on potential complications.[11,12,25,28–30]

Table 2. Computed Tomography Image Quality and Artifacts of Studied Prosthetic Heart Valves

		Artifacts				Image Quality: (Peri)Prosthetic				Image Quality: Leaflets			
Valves	Type	None	Minor	Moderate	Severe	ND	Fair	Good	Excellent	ND	Fair	Good	Excellent
Stentless valves*[25,35,37]	B	●	…	…	…	…	…	…	●	…	●	…	…
Carbomedics[11,12,35–38,40]	BM	●	●	…	…	…	…	●	●	…	…	…	●
ON-X[12,28,35,37,40]	BM	●	●	…	…	…	…	●	●	…	…	…	●
St. Jude Standard[28]	BM†	●	●	…	…	…	…	…	…	…	…	…	…
Medtronic Mosaic[25,35,37]	B	…	●	…	…	…	…	…	●	…	●	●	…
Mitroflow[35,37]	B	…	●	…	…	…	●	●	…	…	●	…	…
St. Jude Epic[35,37]	B	…	●	…	…	…	…	●	●	●	●	…	…
CE Perimount/Magna[25,28,35,37]	B	…	●	●	…	…	…	●	●		●	…	…
ATS[28,38]	BM	…	●	●	…	…	…	…	…	…	…	…	●
St. Jude Regent[28,38]	BM	…	●	●	…	…	…	…	…	…	…	…	●
St. Jude unspecified[12,35–38]	BM	…	●	●	…	…	…	●	…	…	…	●	●
Duromedics[11,35,37]	BM†	…	…	●	…	…	●	●	…	…	…	●	
Sorin bicarbon[11,35,37]	BM	…	…	●	…	…	…	●	●	…	…		●
St. Jude HP[28,40]	BM	…	…	●	…	…	…	●	…	…	…		●
Omnicarbon[38]	MM†	…	…	●	…	…	…		…	…	…		●
Medtronic Hall[11,12,35,37,40]	MM†	●	●	●	…	…	…	●	…	…	…	●	●
Björk-Shiley[11,12,35–38,40]	MM†	…	…	…	●	●	…	…	…	●	…	…	…
Sorin[35–37]	MM†	…	…	…	●	●	…	…	…	●	●	…	…
Medtronic Intact[35]	B	…	…	…	…	…		●	…	●	●	…	…

Image quality was assessed using similar 4- to 5-point scales[35,36,38,40,41] or by volumetric artifact quantification.[26] The remaining studies reported the artifact extent and whether prosthetic heart valve (region) evaluation was possible. Image quality is summarized in this table as nondiagnostic, fair, good, and excellent and artifacts as: none, minor, moderate, and severe. B indicates biological; BM, bileaflet mechanical; CB, caged-ball; MM, monoleaflet mechanical; and ND, nondiagnostic.

*Medtronic Freestyle, St. Jude Toronto, and Sorin Freedom Solo.

†Valve types have been discontinued.

Image Quality

Depending on the type of components, PHVs can cause hyperdense (blooming and bright streak) or hypodense (beam-hardening and dark streak) artifacts that may affect image quality (Figure 2). In vitro, artifact reduction was achieved with prospective ECG-triggering when compared with retrospective ECG-gating[31] and with increased tube voltage (140 versus 100–120 kV).[32] Iterative reconstruction techniques allowed 50% to 75% dose reduction[33] and improved objective image quality.[34] Preprocessing filters improved bioprosthetic image quality, and semiautomatic segmentation methods allowed degenerated valve tissue discrimination.[30]

In total, 10 patient studies evaluated 307 mechanical[11,12,24,28,35–38] and 151 biological PHVs.[25,28,35,37,39] For most mechanical valves, image quality was excellent for leaflets and good to excellent for periprosthetic regions (Table 2). Artifacts were least in closed valve position and increased with rapid leaflet motion.[26] Sorin and Björk-Shiley monoleaflet valves consistently displayed severe artifacts related to their cobalt-chrome components, precluding assessment in 14 of 15 and 4 of 7 patients, respectively.[12,35–38] Compared with fluoroscopy, nonenhanced CT showed greater leaflet visibility in 40 unspecified bileaflet valve patients.[24] Results for biological prostheses were less consistent. One study found sufficient image quality for evaluation of 47 of 50 unspecified biological valves.[39] Other studies showed leaflet and periprosthetic image quality to differ strongly between valve types (Table 2).

Magnetic Resonance Imaging

Acquisition

Depending on the clinical context and imaging purpose, different MRI sequences are required including T_1-weighed spin echo and gradient echo sequences, comprising steady-state free-precession and fast gradient echo. Steady-state free-precession is the workhorse sequence for cardiac MRI and provides high blood-tissue contrast allowing biological valve delineation and orifice area assessment.[42] Fast gradient echo is less susceptible to turbulent flow and was used for flow-related artifact reduction.[9,43] Spin echo sequences showed less PHV-related artifacts.[44–47] For flow and velocity measurements, phase-contrast sequences can be used,[48–50] and motion-sensitized acquisitions are being developed to allow turbulent flow assessment.[51] Recently, 4-dimensional (4D) flow MRI was introduced, which may provide quantification and comprehensive characterization of flow patterns and offer insights in hemodynamics after valve replacement.[52]

Image Quality

MRI valve-related artifacts appear as localized signal voids ranging from mild to severe, depending on the amount and type of metal (Figure 3; Table 3).[44,45,53,54] Bileaflet and titanium-containing PHVs caused fewer artifacts than monoleaflet valves or cobalt-chromium alloys.[45,55] PHV artifacts were evaluated in 124 patients with 115 biological and only 10 mechanical valves.[9,43,54,56,57] Signal voids precluded assessment of the mechanical prosthesis itself including the valve leaflets. Biological valves containing a simple ring showed no disturbing artifacts, unlike valves with metal struts.[57] Of 83 patients with various biological valves, 62 showed excellent image quality, 16 moderate, and 5 non-diagnostic because of flow-related artifacts, stent material, arrhythmias, or patient movement.[9,43] One study improved PHV visualization by integrating resonant conduits in experimental setting.[58]

Relevant Risks of CT and MRI

Compared with routine echocardiography, CT and MRI in PHV bear certain risks. The administration of iodinated contrast

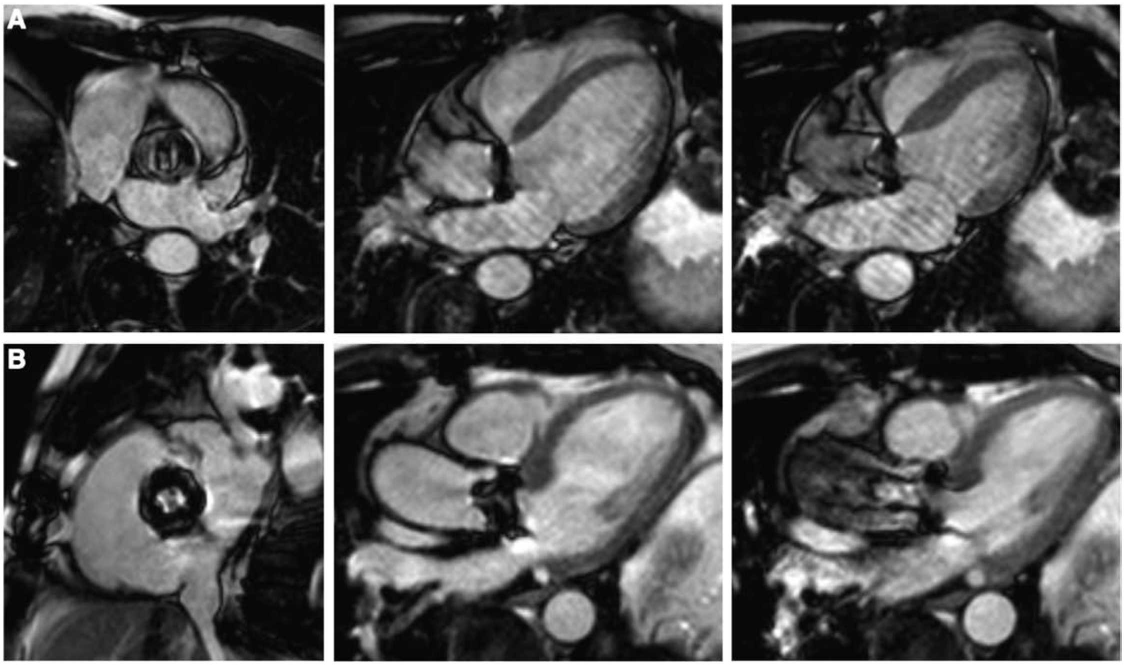

Figure 3. Magnetic resonance imaging in prosthetic heart valves magnetic resonance steady-state free-precession images of the mechanical carbomedics (A, **top** row) and biological Perimount (**B**; **bottom** row) aortic prosthetic valves in plane and perpendicular in diastole and systole, respectively.

Table 3. Magnetic Resonance Imaging Artifacts of Studied Prosthetic Heart Valves

		Artifacts				
Valves	Type	None	Minor	Moderate	Severe	F/L
Hancock Vascor[55]	B*	•	…	…	…	…
St. Jude Toronto SPV[44]	B	…	•	…	…	…
Biocor[44]	B*	…	•	…	…	…
St. Jude bioimplant[46]	B*	…	•	…	…	…
Tascon porcine[44]	B*	…	•	…	…	…
Wessex porcine[44]	B*	…	•	…	…	…
Xenofic pericardial[44]	B*	…	•	…	…	…
Edwards Mira[45,46]	BM*	…	•	…	…	…
CE Porcine[45,54–57]	B	…	•	•	…	…
Hancock Pericardial[46,55,56]	B	…	•	•	…	F/L
Sorin Pericarbon[44]	B	…	•	•	…	
Ionescu-Shiley[54,55]	B*	…	•	•	…	
Sorin bicarbon[46,56]	BM	…	•	•	…	F
St. Jude unspecified[55,56]	BM	…	•	•	…	F
Aortech[44]	MM*	…	•	•	…	…
Medtronic Hall (Kaster)[55,56]	MM*	…	•	•	…	F
Omniscience[46,55]	MM*	…	•	•	…	…
Smeloff-Cutter[44,55,56]	CB*	…	•	•	…	F
ON-X[46]	BM	…	…	•	…	…
Duromedics[56]	BM*	…	…	•	…	F
Lillehei-Kaster[54]	MM*	…	…	•	…	…
Ultracor[46]	MM*	…	…	•	…	…
Medtronic Intact[44]	B	…	•	•	•	…
Mitroflow[44,46]	B	…	•	•	•	…
St. Jude Masters/HP[44,46,54]	BM	…	•	•	•	…
St. Jude Regent[44]	BM	…	•	•	•	…
CE Perimount/Magna[42,45,46,57]	B	…	…	•	•	…
ATS[44]	BM	…	…	•	•	…
Jyros[44]	BM*	…	…	•	•	…
Beall[44]	MM*	…	…	•	•	…
Björk-Shiley[44,46,54–56]	MM*	…	…	•	•	F
Omnicarbon[55]	MM*	…	…	•	•	…
Sorin allcarbon[44]	MM*	…	…	•	•	…
Starr-Edwards[53,55]	CB*	…	…	…	•	…

Artifacts: none, minor=smaller than the prosthesis, moderate=same or slightly larger than prosthesis, severe=larger than prosthesis or precluding assessment of adjacent structures B indicates biological; BM, bileaflet mechanical; CB, caged-ball; F, in vivo flow assessment possible; L, in vivo leaflet assessment possible; and MM, monoleaflet mechanical.

*Valve types have been discontinued.

agents for contrast-enhanced CT may cause adverse reactions including contrast-induced nephropathy. Patients with known contrast medium allergy or impaired renal function may, therefore, not be eligible for contrast-enhanced CT imaging. MRI may entail severe complications related to the presence of metal devices. Pacemakers and implantable cardioverter defibrillators, in general, are an absolute contraindication. MRI safety has extensively been studied at 0.35 to 4.7T in 105 mechanical and 59 biological PHVs.[19,44–46,53–55,59–62] The MRI force exerted on studied PHVs until 4.7T was less than gravity, or the beating heart[45,59,60] and temperature changes (max. +0.7°C) were considered safe as well.[19,44–46,53–55] None of included studies reported incidents related to MRI exposure in patients with PHV. Three 0.5 to 1.5T MRI studies including 115 patients specifically observed no rhythm disturbances, clinical symptoms, discomfort, or safety problems.[47,54,63]

Anatomy and Function

Additional CT imaging can be helpful in the assessment of the periprosthetic anatomy, structural prosthetic integrity, and pathology.[11,18,64] CT has been used to estimate the PHV size and function by evaluating diameters, orifice areas, and leaflet

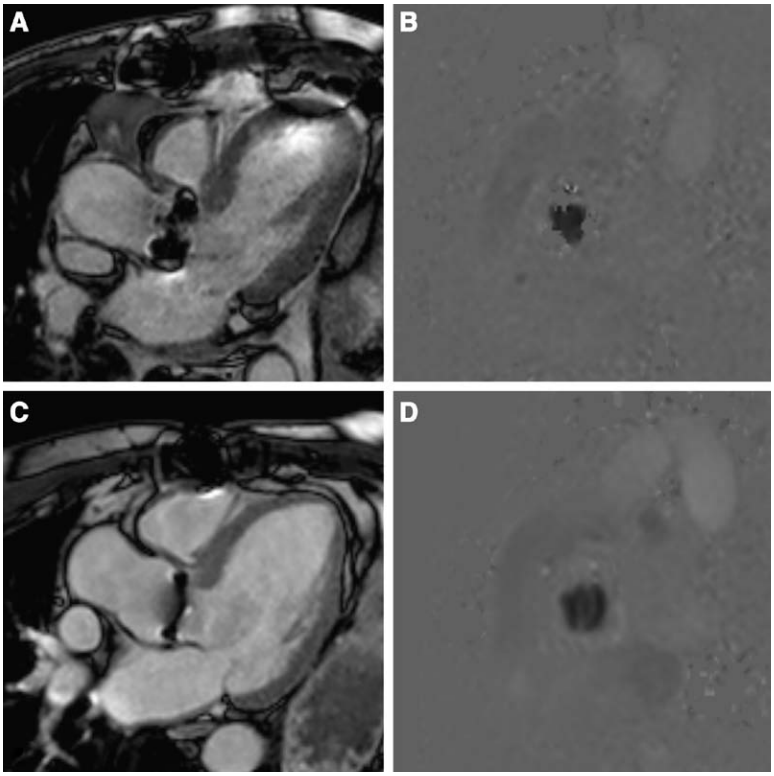

Figure 4. Magnetic resonance imaging flow assessment left ventricular outflow tract steady-state free-precession images (**A** and **C**) and in plane phase-contrast images (**B** and **D**) of a biological Carpentier-Edwards Perimount and a mechanical St. Jude aortic prosthetic heart valve, respectively. Note the single opening orifice of the biological valve (**B**) and the 3 opening orifices of the mechanical valve (**D**).

motion and to measure anatomic dimensions such as the left ventricular outflow tract, sinotubular junction, and coronary ostium heights in biological valves as preassessment for transcatheter valve-in-valve implantation.[57] MRI provided cardiac dimensions including the aortic diameter after mechanical PHV implantation,[13] pulmonary conduit diameter,[65] and ventricular function[66] and allowed assessment of aortic root distensibility and annulus area throughout the cardiac cycle in bioprostheses in animals (n=19)[67] and stentless valves in patients (n=10).[68] MRI and CT showed good agreement for geometric area, aortic root, left ventricular outflow tract, and annulus diameter measurements in patients with bioprostheses (max. mean difference, 1.4±2.3 mm).[57] Furthermore, MRI phantom studies extensively evaluated normal PHV flow patterns, which depended on valve size, design, vessel geometry, and distance of downstream measurements.[21,42,48,49,51,69–73] In animals, flow patterns were also affected by prosthesis type[74] and orientation.[75] In patients, mechanical valves demonstrated more skewed and complex flow patterns.[13,48,52,70,76] Stented and smaller PHVs showed greater velocities than stentless and larger valves.[42,69,77] Velocity measurements were performed ≥1.0 valve diameter downstream for flow and motion artifacts[13,15,48,76] although mitral prostheses showed no significant flow artifacts.[43] Valve-related signal loss hampered Starr-Edwards flow assessment at <40 mm downstream.[21] Only 2 studies performed measurements at 0.25 diameter downstream.[70,71] Laser Doppler anemometry and MRI showed good agreement (<15% difference) for vessel center velocity measurements.[70,71,73] Furthermore, in vitro MRI phase-contrast measurements showed excellent correlation with the flow transducer (reference test).[72] Phase-contrast MRI (Figure 4) was used in 1 study in addition to TTE as standard work-up after valve surgery.[78] A single study visualized flow profiles in time with 4D flow and successfully assessed jet eccentricity and hemodynamic vortex formation from the sinotubular junction onward.[52]

Pathology

Structural Deterioration

In aortic valves, the effective valve orifice area (EOA) estimated with TTE is used as a measure for stenosis evaluation. CT planimetric geometric orifice area (GOA) and TTE functional EOA measurements are distinct noninterchangeable entities.[79] Nevertheless, several studies compared them.[25,39,80] For biological valves, the leaflet GOA was measured in maximal systolic phase in 100 patients[25,39] and correlated well with the EOA.[25] CT detected moderate stenosis using the GOA,[39] but the GOA was consistently higher than the EOA (mean, 0.06 cm2).[25,39] Aortic biological valve degeneration was evaluated in 5 CT studies.[25,39,81–83] Despite the variable leaflet image quality, 1 study detected restricted leaflet opening in all 34 patients with severe bioprosthetic dysfunction (EOA <0.65 cm2/m^2).[25] CT also detected thickened leaflets (Figure 5) and hypoattenuating masses related to thrombus formation[25] and visualized valve ring or leaflet calcifications.[39,81–83] Degenerative valves showed higher CT calcification volumes (181±33 mm^3) when compared with nondegenerative (75±37 mm^3) valves[82,83] and were significantly associated with patient–prosthesis mismatch and higher TTE transprosthetic gradients and regurgitation.[83] CT also allowed evaluation of pulmonary tissue-engineered[84,85] and stentless[86] valve morphology.

For MRI, the measured aortic biological GOA (Figure 6) was within the EOA SDs,[42] despite the fundamental differences discussed, and showed strong agreement between MRI

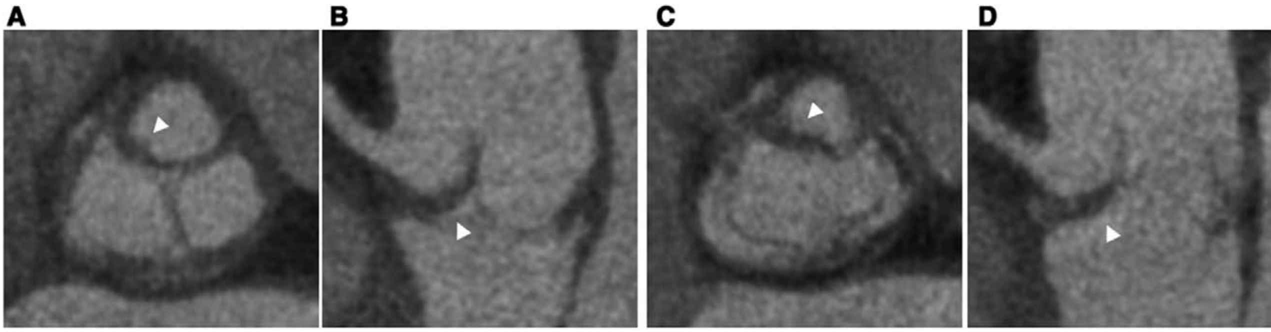

Figure 5. Structural valve deterioration computed tomographic (CT) images of a Sorin Freedom Solo stentless 23-mm bioprosthesis in aortic position. Note the thickening of the right coronary cusp (arrowheads) presented in systole (**A** and **B**) and the in diastole (**C** and **D**) with leaflet opening restriction.

and TTE (mean difference, 0.02±0.24 cm^2) and MRI and TEE (mean difference, 0.05±0.15 cm^2) in 65 patients.[9] For mitral GOA, MRI overestimated the echocardiographic EOA in all PHV types,[72] and a mean difference of 0.06±0.11 cm^2 was reported.[43] Despite atrial fibrillation, mitral measurements could be obtained successfully.[43]

MRI detected stenosis in 12 of 17 patients with tissue-engineered pulmonary valves by showing high peak velocities (3.5–4.0 m/s) and mild to severe insufficiency (10%–40%).[50] In addition, MRI allowed cusp motion evaluation in tissue-engineered and biological left- and right-sided PHVs in sheep[65] and man[43,66,87] and detected leaflet restriction.[43,65] Moreover, significant wall thickening and PHV-conduit enhancement were visualized in all stenosis patients, which correlated histologically with severe inflammation and fibrosis.

Regurgitation

Important for patient follow-up is evaluation of regurgitation (Figure 7A and 7B). When compared with TTE, CT performance for detecting aortic biological valve regurgitation was poor.[39] Periprosthetic regurgitation (nonendocarditis) in mechanical valves was detected by CT and echocardiography in 10 cases.[11,12,28] Selected CT protocols did allow discrimination of periprosthetic contrast-enhanced blood from surgical Teflon pledgets.[88]

The performance of MRI, compared with TEE, was systematically assessed by 1 group in 47 unique patients with 48 mechanical and 7 biological valves.[47,89] Physiological regurgitation was found in 17 of 55 PHVs, and both modalities detected regurgitation missed by the other technique in 4 (MRI) and 5 (TEE) patients.[89] Pathological regurgitation introduced more signal loss or turbulence and showed greater insufficiency jets.[47,56,89] MRI distinguished periprosthetic from transprosthetic regurgitation in all, but disagreed with TEE in 4 aortic valves.[89] TEE was unable to detect the origin of regurgitation in 2 PHVs. Surgical confirmation showed that MRI was correct in 11 of 13 and TEE in 12 of 13 patients. MRI regurgitation quantification correlated well with TEE, despite overestimation (4/32) and underestimation (3/32) of TEE classifications. For pulmonary PHVs, MRI was used in 144 patients to assess follow-up regurgitation and regurgitation fractions.[66,90–92] MRI distinguished minimal and mild pulmonary valve incompetence better than echocardiography (n=13).[90] In 20 patients, MRI was also used to assess forward flow in biological pulmonary PHVs.[93]

Prosthetic Valve Endocarditis

Endocarditis detection was systematically evaluated in 3 CT studies including 61 patients with 31 mechanical and 30 biological PHVs.[17,18,94] Two studies found no advantage over TEE for vegetation detection, irrespective of valve type.[17,18] In a third

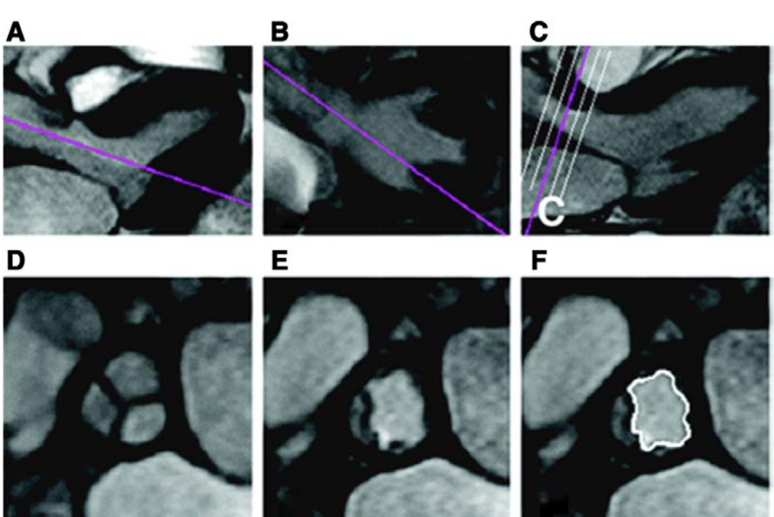

Figure 6. Assessment of the geometric orifice area magnetic resonance views of the left ventricular outflow tract (**A**–**C**) are used to reconstruct images perpendicular to the transprosthetic flow jet of a biological aortic prosthetic valve in diastole (**D**) and systole (**E**). The prosthetic geometric orifice area is derived by planimetry of the greatest orifice in systole (**F**). Reproduced from von Knobelsdorff-Brenkenhoff et al[9] with permission of the publisher. Copyright @ 2009, Wolters Kluwer Health Inc.

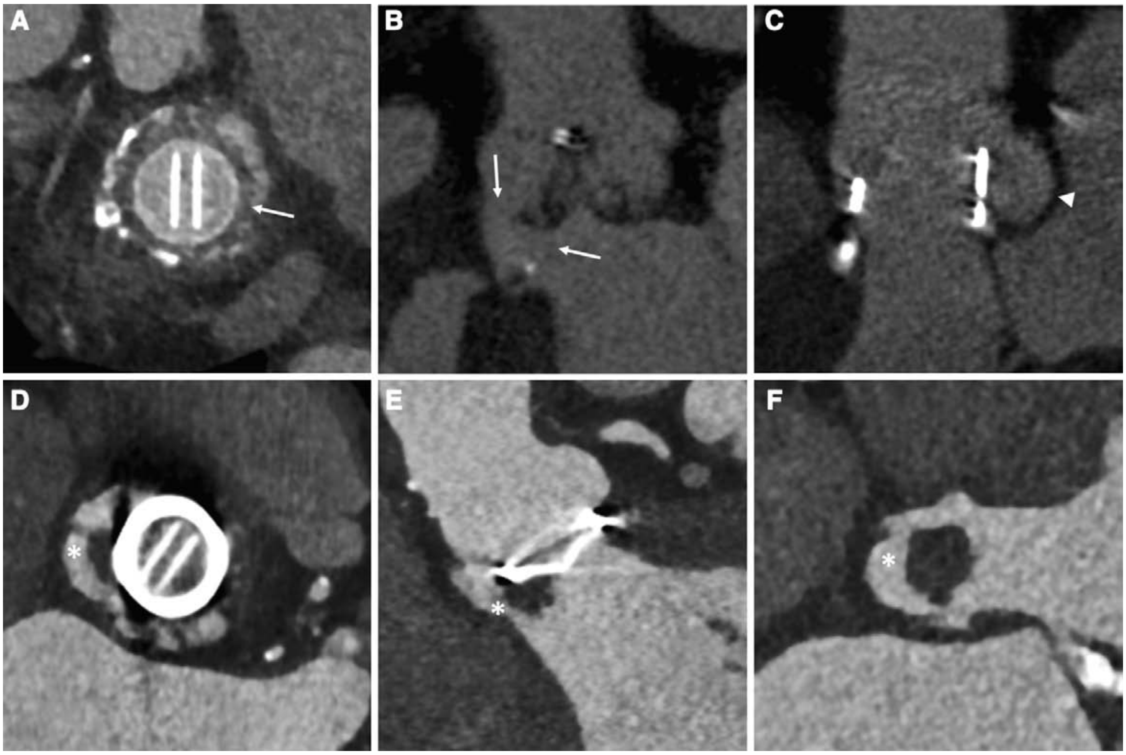

Figure 7. Computed tomography (CT) in periprosthetic leakage and prosthetic valve endocarditis. **A**, Periprosthetic leakage (arrows) in a patient with the mechanical St. Jude valve. **B**, Periprosthetic leakage (arrows) in a patient with the Medtronic Mosaic valve. **C**, Pseudoaneurysm (arrows) in a patient with the Perimount biological prosthesis. **D**–**F**, Endocarditis in a patient with a mechanical St. Jude prosthesis in aortic position. CT showed a large vegetation and provided information on mycotic aneurysm extension (**D**, short-axis view: valve level; **E**, perpendicular plane: valve level; **F**, short-axis view: subprosthetic level).

study, CT detected vegetations missed by echocardiography in 2 biological and 1 mechanical PHV.[94] CT was better in depicting mycotic aneurysms and abscesses when compared with TTE/TEE (11 versus 4, not detected by the other modality).[17,94] Moreover, CT provided surgically relevant additional information on aneurysm extension,[18,94] changed the treatment to surgery (n=1) and resulted in an alternative surgical strategy (n=6).[94] Figure 7D to 7F shows an example of CT in endocarditis. Altogether, diagnosis in patients suspected of PHV endocarditis was most accurate when CT and TEE were combined.[17,94] MRI performance was not studied in patients with suspected PHV endocarditis.

Thrombosis and Pannus Formation

One of the main findings in suspected PHV obstruction is restricted leaflet motion. CT was highly accurate in measuring mechanical leaflet angles in normal and restricted valves and showed a maximal in vitro difference between CT and fluoroscopy of 2°.[95] A good correlation between CT and fluoroscopy leaflet angles was also found in 3 patient studies (n=101),[10,24,36] and bileaflet valve angles corresponded to the manufacturers' data.[36,96] For monoleaflet valves, CT did not allow angle measurements in 6 of 7 Björk-Shileys[36,38] and slightly underestimated Medtronic Hall opening angles (67° versus 75° by manufacturer).[10] Fluoroscopy did not allow angle measurements in 8 of 115 patients (because of high heart rate or difficult beam positioning) and was incorrect in 5 of 115 cases.[10,11,24]

Suspected mechanical PHV obstruction was systematically evaluated using CT in 70 patients.[11,12,64,97,98] CT detected the morphological substrate of obstruction in 21 of 25 selected

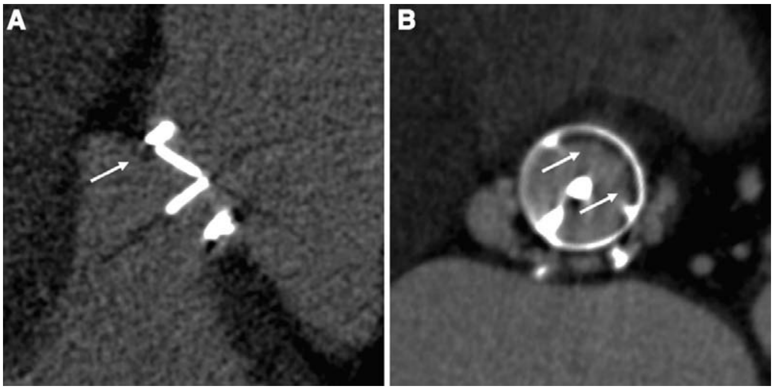

Figure 8. Prosthetic valve pathology detected with computed tomography. **A**, Obstruction of an ATS mitral valve because of hypodense tissue (arrow) based on thrombus formation. **B**, Pannus tissue (arrows) underneath a Medtronic Hall monoleaflet valve.

Table 4. Role of CT and MRI for Prosthetic Heart Valve Evaluation

Indication	Modality	Potentials	Notes
Baseline	CT	Provide overview of cardiac anatomy and prosthesis related structures	Periprosthetic image quality valve type dependent
		Assess prosthetic inner diameter	…
		Assess prosthetic GOA	Planimetric measurements, not interchangeable with EOA
		Measure leaflet opening and closing angles for mechanical valves	Poor image quality in Björk-Shiley monoleaflet valves
		Assess overall leaflet motion for some biological valves	Only if leaflets visible
	MRI	Assess cardiac dimensions and GOA in specific biological prostheses	…
Suspected dysfunction	CT	Detect restricted leaflet excursions independent of valve orientation or position	…
Obstruction	CT	Detect the morphological substrate of valve obstruction	Limited value for the Sorin and Björk-Shiley monoleaflets
	MRI	Measure velocities and detect abnormal flow patterns	…
Thrombus	CT	Detect subprosthetic or supraprosthetic mass, often attached to leaflet and restricted leaflet motion	Tissue differentiation based on CT attenuation not yet established
Pannus	CT	Detect (semi)circular subprosthetic mass along valve ring, mostly attached to the pivot guard, leaflet function may be normal	Tissue differentiation based on CT attenuation not yet established
Second prosthesis	CT	Detect LVOT obstruction by protruding mitral prosthesis	…
Prosthesis angulation	CT	Detect angulated position of implanted prosthesis in relation to LVOT	…
Patient–prosthesis mismatch	CT	Support echocardiography diagnosis by showing normal leaflet function, absent masses and small GOA	…
Bioprosthesis degeneration	CT	Detect leaflet thickening	…
		Detect leaflet and valve calcifications	…
		Show distribution of calcifications	…
	MRI	Assess overall biological valve leaflet motion and detect restricted leaflets	Only if leaflets visible
Paraprosthetic regurgitation	CT	Limited, detect contrast agent extravasation in combination with echocardiography	Sensitivity of CT alone is moderate
	MRI	Detect paraprosthetic regurgitation	TEE required
Regurgitation	CT	Limited	Poor CT performance
	MRI	Detect valvular regurgitation and quantify regurgitation fraction	Clinically used for pulmonary biological prostheses
Endocarditis	CT	Limited, detect vegetations in combination with echocardiography	Sensitivity of CT alone is moderate
		Detect mycotic aneurysms and their extent	…
Valve dehiscence	CT	Detect valve dehiscence	…
Pseudoaneurysm	CT	Detect pseudoaneurysm formation and show their extent	…
Pre surgical procedure	CT	Evaluate anatomic structures and pathology extent relevant for surgical planning including coronary arteries and relation of the bypass grafts to sternum	…
Pre valve-in-valve procedure	CT	Measure aortic root, LVOT, bioprosthetic diameter, coronary ostia height	…

CT indicates computed tomography; EOA, effective orifice area; GOA, geometric orifice area; LVOT, left ventricular outflow tract; MRI, magnetic resonance imaging; and TEE, transesophageal echocardiography.

patients with surgical confirmation in 18.[11,12,64] Of those, 16 patients showed a subprosthetic mass from the interventricular septum to the pivot guard defined as pannus (n=12), pannus and thrombus (n=3), or a calcified rim (n=1), and 2 patients showed left ventricular outflow tract obstruction by a mitral PHV. In 1 patient with an increased transprosthetic gradient, CT showed a tilted PHV position.[11] An example is presented in Figure 8. Another group evaluated patients with obstructed aortic valves (based on TTE/fluoroscopy) and detected pannus using CT in 19 of 23 patients and 7 of 29 controls[97,98] and thrombus in 3 of 7 selected patients.[98] Pannus and thrombus were confirmed in all reoperated cases (n=6 and n=2, respectively).[97,98] In contrast, echocardiography only detected an obstructive mass in 2 of 13 patients with CT masses.[98] It is, however, unclear whether CT allows discrimination of pannus and thrombus based on attenuation values. Pannus had a significantly higher mean CT attenuation than the interventricular septum in 1 study[64] (170 and 108 HU, respectively) but equal attenuation in another.[97] A mean attenuation values for pannus of 153 HU (n=9) and of 60 and 99 HU for thrombus (n=2) were also reported.[98] Moreover, no attenuation difference was found between pure pannus (n=3) and pannus with thrombus (n=2).[11]

CT could support patient–prosthesis mismatch diagnosis in 10 patients with mechanical valves by showing a normal PHV function and small GOA, in combination with a small EOA (TTE).[80] The correlation between mechanical GOA and EOA in 41 patients was moderate, and mean GOA was 1.4 cm^2 higher.[80] Overall, CT measurements of the prosthetic diameter (internal and external)[10,24,96] and GOA[10,96] correlated well with the manufacturer specifications and between readers in mechanical valves. The correlation for both diameter and GOA was better with sinus rhythm and for aortic when compared with mitral valves.[10,96] Motion artifacts precluded CT measurements in 6 PHVs.[10]

MRI was able to distinguish restricted from normal PHVs in vitro by central/lateral velocity jet ratios at low and high flow rates, whereas transprosthetic gradients were only discriminative at high flow rates.[14] Restricted valves showed higher velocities, merged or far-reaching asymmetrical jets, and reversed flow in the stenosed region.[21,51,73] Because of high velocities, flow measurements were less accurate and often only possible at 40 mm downstream.[21] Still, velocity measurements showed good agreement with laser Doppler anemometry for the Björk-Shiley and St Jude valve.[73] No MRI study reported on the evaluation of pannus or thrombus using MRI.

Considerations

Patient selection and study methods differ considerably between most studies, which makes head-to-head comparison of results difficult. For instance, MRI studies were published between 1985 and 2015 using different field strengths (0.2–3.0T) and acquisition sequences. MRI acquisition has changed and improved significantly over the years, and many PHVs studied in the early years have been discontinued. Hence, their specific image quality is less relevant in the present clinical practice. Furthermore, most study sample sizes are small because of the relatively low incidence of complications in patients with PHVs. Results presented thus show clinical relevance for specific PHVs, patients, or complications. Also, several studies excluded patients with impaired left ventricular function, arrhythmias, impaired renal function, clinically unstable patients, or patients in whom echocardiography was not possible. On the basis of available results, we have summarized the potentials of CT and MRI for clinical PHV assessment in Table 4.

Conclusions

The use for newer imaging modalities for the evaluation of PHVs may be given in by the limitations of current techniques. For example, echocardiography may not detect abnormalities because of acoustic shadowing caused by prosthetic components and limited viewing planes. CT and MRI may provide incremental information in selected patients by uncoupling image analysis and acquisition and providing a complete anatomic overview. CT can identify morphological correlates of obstruction such as (peri)prosthetic masses, restricted leaflet motion, left ventricular outflow tract obstruction, and thickening and calcification of leaflets, which could be of importance for valve-in-valve procedures. Although no clear advantage over echocardiography was found for the detection of vegetations and periprosthetic regurgitation in general, CT showed incremental value for the assessment of endocarditis extension (pseudoaneurysms and valve dehiscence). Hence, the most important clinical indications in which CT provides additional information to echocardiography are suspected PHV obstruction in mechanical valves, as well as endocarditis in biological and mechanical valves. Limitations for CT evaluation are excessive metal artifacts caused by older mechanical cobalt-chromium PHVs and limited visibility of normal biological leaflets. In addition, arrhythmias and high heart rates may impair image quality or induce artifacts. Experimental studies demonstrated promising results for artifact and radiation dose reduction although no clinical studies have been performed to assess these results in patients.

MRI has shown to be safe and overall PHV-related artifacts remained localized, but mechanical details of the PHV could not be assessed. MRI allowed annular and orifice area measurements in biological valves with good agreement to echocardiography and assessment of flow and velocity patterns in biological and mechanical valves. MRI may potentially demonstrate abnormal asymmetrical flow patterns in PHV obstruction although leaflet angle measurements may not be possible. No studies have been published on the diagnostic performance for detecting PHV abnormalities such as pseudoaneurysms and abscesses. However, MRI was a useful tool for regurgitation assessment, especially in the follow-up of pulmonary valves.

Additional studies in nonselected populations may further specify the usefulness for CT or MRI in the overall PHV population. Contemporary studies are mandatory to optimize acquisition protocols and to present reference values to discriminate normal from pathological conditions for clinical implementation.

Sources of Funding

This study was funded by the Dutch Heart Foundation, The Netherlands (grants 2009B014 and 2013T071).

Disclosures

Prof dr van Herwerden is a clinical research consultant for St. Jude Medical Inc, St. Paul, USA. The other authors report no conflicts.

References

1. Yacoub MH, Takkenberg JJ. Will heart valve tissue engineering change the world? *Nat Clin Pract Cardiovasc Med*. 2005;2:60–61. doi: 10.1038/ncpcardio0112.
2. Hammermeister K, Sethi GK, Henderson WG, Grover FL, Oprian C, Rahimtoola SH. Outcomes 15 years after valve replacement with a mechanical versus a bioprosthetic valve: final report of the Veterans Affairs

randomized trial. *J Am Coll Cardiol*. 2000;36:1152–1158. doi: 10.1016/S0735-1097(00)00834-2.

3. Vongpatanasin W, Hillis LD, Lange RA. Prosthetic heart valves. *N Engl J Med*. 1996;335:407–416. doi: 10.1056/NEJM199608083350607.
4. Zoghbi WA, Chambers JB, Dumesnil JG, Foster E, Gottdiener JS, Grayburn PA, Khandheria BK, Levine RA, Marx GR, Miller FA Jr, Nakatani S, Quiñones MA, Rakowski H, Rodriguez LL, Swaminathan M, Waggoner AD, Weissman NJ, Zabalgoitia M; American Society of Echocardiography's Guidelines and Standards Committee; Task Force on Prosthetic Valves; American College of Cardiology Cardiovascular Imaging Committee; Cardiac Imaging Committee of the American Heart Association; European Association of Echocardiography; European Society of Cardiology; Japanese Society of Echocardiography; Canadian Society of Echocardiography; American College of Cardiology Foundation; American Heart Association; European Association of Echocardiography; European Society of Cardiology; Japanese Society of Echocardiography; Canadian Society of Echocardiography. Recommendations for evaluation of prosthetic valves with echocardiography and doppler ultrasound: a report From the American Society of Echocardiography's Guidelines and Standards Committee and the Task Force on Prosthetic Valves, developed in conjunction with the American College of Cardiology Cardiovascular Imaging Committee, Cardiac Imaging Committee of the American Heart Association, the European Association of Echocardiography, a registered branch of the European Society of Cardiology, the Japanese Society of Echocardiography and the Canadian Society of Echocardiography, endorsed by the American College of Cardiology Foundation, American Heart Association, European Association of Echocardiography, a registered branch of the European Society of Cardiology, the Japanese Society of Echocardiography, and Canadian Society of Echocardiography. *J Am Soc Echocardiogr*. 2009;22:975–1014; quiz 1082. doi: 10.1016/j.echo.2009.07.013.
5. Girard SE, Miller FA Jr, Orszulak TA, Mullany CJ, Montgomery S, Edwards WD, Tazelaar HD, Malouf JF, Tajik AJ. Reoperation for prosthetic aortic valve obstruction in the era of echocardiography: trends in diagnostic testing and comparison with surgical findings. *J Am Coll Cardiol*. 2001;37:579–584.
6. Faletra F, Constantin C, De Chiara F, Masciocco G, Santambrogio G, Moreo A, Alberti A, Vitali E, Pellegrini A. Incorrect echocardiographic diagnosis in patients with mechanical prosthetic valve dysfunction: correlation with surgical findings. *Am J Med*. 2000;108:531–537.
7. Habets J, Tanis W, Reitsma JB, van den Brink RB, Mali WP, Chamuleau SA, Budde RP. Are novel non-invasive imaging techniques needed in patients with suspected prosthetic heart valve endocarditis? A systematic review and meta-analysis. *Eur Radiol*. 2015;25:2125–2133. doi: 10.1007/s00330-015-3605-7.
8. Tanis W, Habets J, van den Brink RB, Symersky P, Budde RP, Chamuleau SA. Differentiation of thrombus from pannus as the cause of acquired mechanical prosthetic heart valve obstruction by non-invasive imaging: a review of the literature. *Eur Heart J Cardiovasc Imaging*. 2014;15:119–129. doi: 10.1093/ehjci/jet127.
9. von Knobelsdorff-Brenkenhoff F, Rudolph A, Wassmuth R, Bohl S, Buschmann EE, Abdel-Aty H, Dietz R, Schulz-Menger J. Feasibility of cardiovascular magnetic resonance to assess the orifice area of aortic bioprostheses. *Circ Cardiovasc Imaging*. 2009;2:397–404, 2 p following 404. doi: 10.1161/CIRCIMAGING.108.840967.
10. LaBounty TM, Agarwal PP, Chughtai A, Bach DS, Wizauer E, Kazerooni EA. Evaluation of mechanical heart valve size and function with ECG-gated 64-MDCT. *AJR Am J Roentgenol*. 2009;193:W389–W396. doi: 10.2214/AJR.08.2178.
11. Symersky P, Budde RP, de Mol BA, Prokop M. Comparison of multidetector-row computed tomography to echocardiography and fluoroscopy for evaluation of patients with mechanical prosthetic valve obstruction. *Am J Cardiol*. 2009;104:1128–1134. doi: 10.1016/j.amjcard.2009.05.061.
12. Tsai IC, Lin YK, Chang Y, Fu YC, Wang CC, Hsieh SR, Wei HJ, Tsai HW, Jan SL, Wang KY, Chen MC, Chen CC. Correctness of multi-detector-row computed tomography for diagnosing mechanical prosthetic heart valve disorders using operative findings as a gold standard. *Eur Radiol*. 2009;19:857–867. doi: 10.1007/s00330-008-1232-2.
13. Botnar R, Nagel E, Scheidegger MB, Pedersen EM, Hess O, Boesiger P. Assessment of prosthetic aortic valve performance by magnetic resonance velocity imaging. *MAGMA*. 2000;10:18–26.
14. Garcia J, Marrufo O, Rodriguez AO, Pibarot P, Kadem L. A new index measured by cardiovascular magnetic resonance imaging to detect mechanical heart valve malfunction. *Conf Proc IEEE Eng Med Biol Soc*. 2011;2011:1347–1350. doi: 10.1109/IEMBS.2011.6090317.
15. Pennekamp W, Geyhan N, Soeren P, Volkmar N. Determination of flow profiles of different mechanical aortic valve prostheses using phase-contrast MRI. *J Cardiovasc Surg (Torino)*. 2011;52:277–284.
16. Liberati A, Altman DG, Tetzlaff J, Mulrow C, Gøtzsche PC, Ioannidis JP, Clarke M, Devereaux PJ, Kleijnen J, Moher D. The PRISMA statement for reporting systematic reviews and meta-analyses of studies that evaluate healthcare interventions: explanation and elaboration. *BMJ*. 2009;339:b2700. doi: 10.1136/bmj.b2700.
17. Fagman E, Perrotta S, Bech-Hanssen O, Flinck A, Lamm C, Olaison L, Svensson G. ECG-gated computed tomography: a new role for patients with suspected aortic prosthetic valve endocarditis. *Eur Radiol*. 2012;22:2407–2414. doi: 10.1007/s00330-012-2491-5.
18. Feuchtner GM, Stolzmann P, Dichtl W, Schertler T, Bonatti J, Scheffel H, Mueller S, Plass A, Mueller L, Bartel T, Wolf F, Alkadhi H. Multislice computed tomography in infective endocarditis: comparison with transesophageal echocardiography and intraoperative findings. *J Am Coll Cardiol*. 2009;53:436–444. doi: 10.1016/j.jacc.2008.01.077.
19. Frank H, Buxbaum P, Huber L, Globits S, Glogar D, Wolner E, Mayr H, Imhof H. In vitro behaviour of mechanical heart valves in a 1.5 t superconducting magnet. *Eur Radiol*. 1992;2:555–558. doi: 10.1007/BF00187551.
20. Gurvitch R, Wood DA, Tay EL, Leipsic J, Ye J, Lichtenstein SV, Thompson CR, Carere RG, Wijesinghe N, Nietlispach F, Boone RH, Lauck S, Cheung A, Webb JG. Transcatheter aortic valve implantation: durability of clinical and hemodynamic outcomes beyond 3 years in a large patient cohort. *Circulation*. 2010;122:1319–1327. doi: 10.1161/CIRCULATIONAHA.110.948877.
21. Walker PG, Pedersen EM, Oyre S, Flepp L, Ringgaard S, Heinrich RS, Walton SP, Hasenkam JM, Jorgensen HS, Yoganathan AP. Magnetic resonance velocity imaging: a new method for prosthetic heart valve study. *J Heart Valve Dis*. 1995;4:296–307.
22. Nishimura RA, Otto CM, Bonow RO, Carabello BA, Erwin JP III, Guyton RA, O'Gara PT, Ruiz CE, Skubas NJ, Sorajja P, Sundt TM III, Thomas JD; American College of Cardiology/American Heart Association Task Force on Practice Guidelines. 2014 AHA/ACC guideline for the management of patients with valvular heart disease: executive summary: a report of the American College of Cardiology/American Heart Association Task Force on Practice Guidelines. *J Am Coll Cardiol*. 2014;63:2438–2488. doi: 10.1016/j.jacc.2014.02.537.
23. Vahanian A, Alfieri O, Andreotti F, Antunes MJ, Barón-Esquivias G, Baumgartner H, Borger MA, Carrel TP, De Bonis M, Evangelista A, Falk V, Lung B, Lancellotti P, Pierard L, Price S, Schäfers HJ, Schuler G, Stepinska J, Swedberg K, Takkenberg J, Von Oppell UO, Windecker S, Zamorano JL, Zembala M; ESC Committee for Practice Guidelines (CPG); Joint Task Force on the Management of Valvular Heart Disease of the European Society of Cardiology (ESC); European Association for Cardio-Thoracic Surgery (EACTS). Guidelines on the management of valvular heart disease (version 2012): the Joint Task Force on the Management of Valvular Heart Disease of the European Society of Cardiology (ESC) and the European Association for Cardio-Thoracic Surgery (EACTS). *Eur J Cardiothorac Surg*. 2012;42:S1–44. doi: 10.1093/ejcts/ezs455.
24. Bazeed MF, Moselhy MS, Rezk AI, Al-Murayeh MA. Low radiation dose non-contrast cardiac CT: is it of value in the evaluation of mechanical aortic valve. *Acta Radiol*. 2012;53:389–393. doi: 10.1258/ar.2012.110253.
25. Chenot F, Montant P, Goffinet C, Pasquet A, Vancraeynest D, Coche E, Vanoverschelde JL, Gerber BL. Evaluation of anatomic valve opening and leaflet morphology in aortic valve bioprosthesis by using multidetector CT: comparison with transthoracic echocardiography. *Radiology*. 2010;255:377–385. doi: 10.1148/radiol.0000082294.
26. Symersky P, Budde RP, Westers P, de Mol BA, Prokop M. Multidetector CT imaging of mechanical prosthetic heart valves: quantification of artifacts with a pulsatile in-vitro model. *Eur Radiol*. 2011;21:2103–2110. doi: 10.1007/s00330-011-2146-y.
27. Suchá D, Daans CG, Symersky P, Planken RN, Mali WP, van Herwerden LA, Budde RP. Reliability, agreement, and presentation of a reference standard for assessing implanted heart valve sizes by multidetector-row computed tomography. *Am J Cardiol*. 2015;116:112–120. doi: 10.1016/j.amjcard.2015.03.048.
28. Hara M, Nishino M, Taniike M, Makino N, Kato H, Egami Y, Shutta R, Tanouchi J, Hunatsu T, Taniguchi K, Yamada Y. Impact of 64 multi-detector computed tomography for the evaluation of aortic paraprosthetic regurgitation. *J Cardiol*. 2011;58:294–299. doi: 10.1016/j.jjcc.2011.08.002.

29. Tsai IC, Hsieh SR, Chern MS, Huang HT, Chen MC, Tsai WL, Chen CC. Pseudoaneurysm in the left ventricular outflow tract after prosthetic aortic valve implantation: evaluation upon multidetector-row computed tomography. *Tex Heart Inst J*. 2009;36:428–432.
30. Ruggieri VG, Haigron P, Wang Q, Esneault S, Madeleine R, Heautot JF, Leguerrier A, Verhoye JP. CT-scan images preprocessing and segmentation to improve bioprosthesis leaflets morphological analysis. *Med Hypotheses*. 2013;81:86–93. doi: 10.1016/j.mehy.2013.03.032.
31. Symersky P, Habets J, Westers P, de Mol BA, Prokop M, Budde RP. Prospective ECG triggering reduces prosthetic heart valve-induced artefacts compared with retrospective ECG gating on 256-slice CT. *Eur Radiol*. 2012;22:1271–1277. doi: 10.1007/s00330-011-2358-1.
32. Habets J, Symersky P, Leiner T, de Mol BA, Mali WP, Budde RP. Artifact reduction strategies for prosthetic heart valve CT imaging. *Int J Cardiovasc Imaging*. 2012;28:2099–2108. doi: 10.1007/s10554-012-0041-5.
33. Habets J, Symersky P, de Mol BA, Mali WP, Leiner T, Budde RP. A novel iterative reconstruction algorithm allows reduced dose multidetector-row CT imaging of mechanical prosthetic heart valves. *Int J Cardiovasc Imaging*. 2012;28:1567–1575. doi: 10.1007/s10554-011-9954-7.
34. Suchá D, Willemink MJ, de Jong PA, Schilham AM, Leiner T, Symersky P, Budde RP. The impact of a new model-based iterative reconstruction algorithm on prosthetic heart valve related artifacts at reduced radiation dose MDCT. *Int J Cardiovasc Imaging*. 2014;30:785–793. doi: 10.1007/s10554-014-0379-y.
35. Habets J, Symersky P, van Herwerden LA, de Mol BA, Spijkerboer AM, Mali WP, Budde RP. Prosthetic heart valve assessment with multidetector-row CT: imaging characteristics of 91 valves in 83 patients. *Eur Radiol*. 2011;21:1390–1396. doi: 10.1007/s00330-011-2068-8.
36. Konen E, Goitein O, Feinberg MS, Eshet Y, Raanani E, Rimon U, Di-Segni E. The role of ECG-gated MDCT in the evaluation of aortic and mitral mechanical valves: initial experience. *AJR Am J Roentgenol*. 2008;191:26–31. doi: 10.2214/AJR.07.2951.
37. Habets J, van den Brink RB, Uijlings R, Spijkerboer AM, Mali WP, Chamuleau SA, Budde RP. Coronary artery assessment by multidetector computed tomography in patients with prosthetic heart valves. *Eur Radiol*. 2012;22:1278–1286. doi: 10.1007/s00330-011-2360-7.
38. Numata S, Tsutsumi Y, Monta O, Yamazaki S, Seo H, Yoshida S, Samura T, Ohashi H. Mechanical valve evaluation with four-dimensional computed tomography. *J Heart Valve Dis*. 2013;22:837–842.
39. Grünenfelder J, Plass A, Alkadhi H, Genoni M. Evaluation of biological aortic valve prostheses by dual source computer tomography and anatomic measurements for potential transapical valve-in-valve procedure. *Interact Cardiovasc Thorac Surg*. 2008;7:195–199; discussion 199. doi: 10.1510/icvts.2007.166587.
40. Symersky P, Budde RP, Prokop M, de Mol BA. Multidetector-row computed tomography imaging characteristics of mechanical prosthetic valves. *J Heart Valve Dis*. 2011;20:216–222.
41. de Heer LM, Habets J, Kluin J, Stella PR, Mali WP, van Herwerden LA, Budde RP. Assessment of a transcatheter heart valve prosthesis with multidetector computed tomography: *in vitro* and *in vivo* imaging characteristics. *Int J Cardiovasc Imaging*. 2013;29:659–668. doi: 10.1007/s10554-012-0111-8.
42. von Knobelsdorff-Brenkenhoff F, Dieringer MA, Greiser A, Schulz-Menger J. *In vitro* assessment of heart valve bioprostheses by cardiovascular magnetic resonance: four-dimensional mapping of flow patterns and orifice area planimetry. *Eur J Cardiothorac Surg*. 2011;40:736–742. doi: 10.1016/j.ejcts.2010.12.040.
43. von Knobelsdorff-Brenkenhoff F, Rudolph A, Wassmuth R, Schulz-Menger J. Assessment of mitral bioprostheses using cardiovascular magnetic resonance. *J Cardiovasc Magn Reson*. 2010;12:36. doi: 10.1186/1532-429X-12-36.
44. Edwards MB, Taylor KM, Shellock FG. Prosthetic heart valves: evaluation of magnetic field interactions, heating, and artifacts at 1.5 T. *J Magn Reson Imaging*. 2000;12:363–369.
45. Shellock FG. Prosthetic heart valves and annuloplasty rings: assessment of magnetic field interactions, heating, and artifacts at 1.5 Tesla. *J Cardiovasc Magn Reson*. 2001;3:317–324.
46. Pruefer D, Kalden P, Schreiber W, Dahm M, Buerke M, Thelen M, Oelert H. *In vitro* investigation of prosthetic heart valves in magnetic resonance imaging: evaluation of potential hazards. *J Heart Valve Dis*. 2001;10:410–414.
47. Bachmann R, Deutsch HJ, Jüngehülsing M, Sechtem U, Hilger HH, Schicha H. Magnetic resonance tomography in patients with a heart valve prosthesis. *Rofo*. 1991;155:499–505. doi: 10.1055/s-2008-1033306.
48. Hasenkam JM, Ringgaard S, Houlind K, Botnar RM, Stødkilde-Jørgensen H, Boesiger P, Pedersen EM. Prosthetic heart valve evaluation by magnetic resonance imaging. *Eur J Cardiothorac Surg*. 1999;16:300–305.
49. Ringgaard S, Botnar RM, Djurhuus C, Stodkilde-Jorgensen H, Hasenkam JM, Boesiger P, Pedersen EM. High-resolution assessment of velocity fields and shear stresses distal to prosthetic heart valves using high-field magnetic resonance imaging. *J Heart Valve Dis*. 1999;8:96–103.
50. Voges I, Bräsen JH, Entenmann A, Scheid M, Scheewe J, Fischer G, Hart C, Andrade A, Pham HM, Kramer HH, Rickers C. Adverse results of a decellularized tissue-engineered pulmonary valve in humans assessed with magnetic resonance imaging. *Eur J Cardiothorac Surg*. 2013;44:e272–e279. doi: 10.1093/ejcts/ezt328.
51. Adegbite O, Kadem L, Newling B. Purely phase-encoded MRI of turbulent flow through a dysfunctional bileaflet mechanical heart valve. *MAGMA*. 2014;27:227–235. doi: 10.1007/s10334-013-0408-1.
52. von Knobelsdorff-Brenkenhoff F, Trauzeddel RF, Barker AJ, Gruettner H, Markl M, Schulz-Menger J. Blood flow characteristics in the ascending aorta after aortic valve replacement–a pilot study using 4D-flow MRI. *Int J Cardiol*. 2014;170:426–433. doi: 10.1016/j.ijcard.2013.11.034.
53. Soulen RL, Budinger TF, Higgins CB. Magnetic resonance imaging of prosthetic heart valves. *Radiology*. 1985;154:705–707. doi: 10.1148/radiology.154.3.3969474.
54. Randall PA, Kohman LJ, Scalzetti EM, Szeverenyi NM, Panicek DM. Magnetic resonance imaging of prosthetic cardiac valves *in vitro* and in vivo. *Am J Cardiol*. 1988;62:973–976.
55. Hassler M, Le Bas JF, Wolf JE, Contamin C, Waksmann B, Coulomb M. Effects of the magnetic field in magnetic resonance imaging on 15 tested cardiac valve prostheses. *J Radiol*. 1986;67:661–666.
56. Di Cesare E, Enrici RM, Paparoni S, Castaldo F, Alagia MG, Splendiani A, Bottone A, Lupattelli L. Low-field magnetic resonance imaging in the evaluation of mechanical and biological heart valve function. *Eur J Radiol*. 1995;20:224–228.
57. Quail MA, Nordmeyer J, Schievano S, Reinthaler M, Mullen MJ, Taylor AM. Use of cardiovascular magnetic resonance imaging for TAVR assessment in patients with bioprosthetic aortic valves: comparison with computed tomography. *Eur J Radiol*. 2012;81:3912–3917. doi: 10.1016/j.ejrad.2012.07.014.
58. Immel E, Gilbert FJ, Melzer A. Experimental MRI visible resonant prosthetic heart valves. *Minim Invasive Ther Allied Technol*. 2009;18:149–155. doi: 10.1080/13645700902921310.
59. Edwards MB, Ordidge RJ, Hand JW, Taylor KM, Young IR. Assessment of magnetic field (4.7 T) induced forces on prosthetic heart valves and annuloplasty rings. *J Magn Reson Imaging*. 2005;22:311–317. doi: 10.1002/jmri.20373.
60. Edwards MB, Ordidge RJ, Thomas DL, Hand JW, Taylor KM. Translational and rotational forces on heart valve prostheses subjected ex vivo to a 4.7-T MR system. *J Magn Reson Imaging*. 2002;16:653–659. doi: 10.1002/jmri.10201.
61. Shellock FG. Biomedical implants and devices: assessment of magnetic field interactions with a 3.0-Tesla MR system. *J Magn Reson Imaging*. 2002;16:721–732. doi: 10.1002/jmri.10207.
62. Shellock FG, Crues JV. High-field-strength MR imaging and metallic biomedical implants: an ex vivo evaluation of deflection forces. *AJR Am J Roentgenol*. 1988;151:389–392. doi: 10.2214/ajr.151.2.389.
63. Biere L, Pinaud F, Delépine S, Grall S, Viot N, Mateus V, Rouleau F, Corbeau JJ, Prunier F, De Brux JL, Willoteaux S, Furber A. CMR assessment after a transapical-transcatheter aortic valve implantation. *Eur J Radiol*. 2014;83:303–308. doi: 10.1016/j.ejrad.2013.11.007.
64. Ueda T, Teshima H, Fukunaga S, Aoyagi S, Tanaka H. Evaluation of prosthetic valve obstruction on electrocardiographically gated multidetector-row computed tomography–identification of subprosthetic pannus in the aortic position. *Circ J*. 2013;77:418–423.
65. Gottlieb D, Kunal T, Emani S, Aikawa E, Brown DW, Powell AJ, Nedder A, Engelmayr GC Jr, Melero-Martin JM, Sacks MS, Mayer JE Jr. *In vivo* monitoring of function of autologous engineered pulmonary valve. *J Thorac Cardiovasc Surg*. 2010;139:723–731. doi: 10.1016/j.jtcvs.2009.11.006.
66. Lee C, Lee CH, Kwak JG, Song JY, Shim WS, Choi EY, Lee SY, Kim YM. Bicuspid pulmonary valve implantation using polytetrafluoroethylene membrane: early results and assessment of the valve function by magnetic resonance imaging. *Eur J Cardiothorac Surg*. 2013;43:468–472. doi: 10.1093/ejcts/ezs381.
67. Funder JA, Ringgaard S, Frost MW, Wierup P, Klaaborg KE, Hjortdal V, Nygaard H, Hasenkam JM. Aortic root distensibility and cross-sectional areas in stented and subcoronary stentless bioprostheses in pigs.

Interact Cardiovasc Thorac Surg. 2010;10:976–980. doi: 10.1510/icvts.2009.230771.
68. O'Brien MF, Gardner MA, Garlick B, Jalali H, Gordon JA, Whitehouse SL, Strugnell WE, Slaughter R. CryoLife-O'Brien stentless valve: 10-year results of 402 implants. *Ann Thorac Surg*. 2005;79:757–766. doi: 10.1016/j.athoracsur.2004.08.057.
69. Kvitting JP, Dyverfeldt P, Sigfridsson A, Franzén S, Wigström L, Bolger AF, Ebbers T. *In vitro* assessment of flow patterns and turbulence intensity in prosthetic heart valves using generalized phase-contrast MRI. *J Magn Reson Imaging*. 2010;31:1075–1080. doi: 10.1002/jmri.22163.
70. Kozerke S, Hasenkam JM, Nygaard H, Paulsen PK, Pedersen EM, Boesiger P. Heart motion-adapted MR velocity mapping of blood velocity distribution downstream of aortic valve prostheses: initial experience. *Radiology*. 2001;218:548–555. doi: 10.1148/radiology.218.2.r01ja07548.
71. Kozerke S, Hasenkam JM, Pedersen EM, Boesiger P. Visualization of flow patterns distal to aortic valve prostheses in humans using a fast approach for cine 3D velocity mapping. *J Magn Reson Imaging*. 2001;13:690–698.
72. Jackson MS, Igo SR, Lindsey TE, Maragiannis D, Chin KE, Autry K, Schutt Iii R, Shah DJ, Valsecchi P, Kline WB, Little SH. Development of a multi-modality compatible flow loop system for the functional assessment of mitral valve prostheses. *Cardiovasc Eng Technol*. 2014;5:13–24. doi: 10.1007/s13239-014-0177-7
73. Fontaine AA, Heinrich RS, Walker PG, Pedersen EM, Scheidegger MB, Boesiger P, Walton SP, Yoganathan AP. Comparison of magnetic resonance imaging and Laser Doppler Anemometry velocity measurements downstream of replacement heart valves: implications for *in vivo* assessment of prosthetic valve function. *J Heart Valve Dis*. 1996;5:66–73.
74. Funder JA, Frost MW, Ringgaard S, Klaaborg KE, Wierup P, Hjortdal V, Nygaard H, Hasenkam JM. In-vivo blood velocity and velocity gradient profiles downstream of stented and stentless aortic heart valves. *J Heart Valve Dis*. 2010;19:292–303.
75. Mächler H, Reiter G, Perthel M, Reiter U, Bergmann P, Zink M, Rienmüller R, Laas J. Influence of a tilting prosthetic mitral valve orientation on the left ventricular flow - an experimental *in vivo* magnetic resonance imaging study. *Eur J Cardiothorac Surg*. 2007;32:102–107. doi: 10.1016/j.ejcts.2007.02.038.
76. Houlind K, Eschen O, Pedersen EM, Jensen T, Hasenkam JM, Paulsen PK. Magnetic resonance imaging of blood velocity distribution around St. Jude medical aortic valves in patients. *J Heart Valve Dis*. 1996;5:511–517.
77. Matsue H, Sawa Y, Matsumiya G, Matsuda H, Hamada S. Mid-term results of freestyle aortic stentless bioprosthetic valve: clinical impact of quantitative analysis of in-vivo three-dimensional flow velocity profile by magnetic resonance imaging. *J Heart Valve Dis*. 2005;14:630–636.
78. Crouch G, Bennetts J, Sinhal A, Tully PJ, Leong DP, Bradbrook C, Penhall AL, De Pasquale CG, Chakrabarty A, Baker RA, Selvanayagam JB. Early effects of transcatheter aortic valve implantation and aortic valve replacement on myocardial function and aortic valve hemodynamics: insights from cardiovascular magnetic resonance imaging. *J Thorac Cardiovasc Surg*. 2015;149:462–470. doi: 10.1016/j.jtcvs.2014.10.064.
79. Garcia D, Kadem L. What do you mean by aortic valve area: geometric orifice area, effective orifice area, or gorlin area? *J Heart Valve Dis*. 2006;15:601–608.
80. LaBounty TM, Agarwal PP, Chughtai A, Kazerooni EA, Wizauer E, Bach DS. Hemodynamic and functional assessment of mechanical aortic valves using combined echocardiography and multidetector computed tomography. *J Cardiovasc Comput Tomogr*. 2009;3:161–167. doi: 10.1016/j.jcct.2009.03.006.
81. Cereijo JM, Alvarez JR, Quiroga JS, de Alegria AM, Suarez Peñaranda JM. Is distortion of the bioprosthesis ring a risk factor for early calcification? *J Cardiothorac Surg*. 2010;5:77. doi: 10.1186/1749-8090-5-77.
82. Mahjoub H, Mathieu P, Sénéchal M, Larose E, Dumesnil J, Després JP, Pibarot P. ApoB/ApoA-I ratio is associated with increased risk of bioprosthetic valve degeneration. *J Am Coll Cardiol*. 2013;61:752–761. doi: 10.1016/j.jacc.2012.11.033.
83. Mahjoub H, Mathieu P, Larose E, Dahou A, Sénéchal M, Dumesnil JG, Després JP, Pibarot P. Determinants of aortic bioprosthetic valve calcification assessed by multidetector CT. *Heart*. 2015;101:472–477. doi: 10.1136/heartjnl-2014-306445.
84. Dohmen PM, Lembcke A, Holinski S, Kivelitz D, Braun JP, Pruss A, Konertz W. Mid-term clinical results using a tissue-engineered pulmonary valve to reconstruct the right ventricular outflow tract during the Ross procedure. *Ann Thorac Surg*. 2007;84:729–736. doi: 10.1016/j.athoracsur.2007.04.072.
85. Dohmen PM, Lembcke A, Holinski S, Pruss A, Konertz W. Ten years of clinical results with a tissue-engineered pulmonary valve. *Ann Thorac Surg*. 2011;92:1308–1314. doi: 10.1016/j.athoracsur.2011.06.009.
86. Hechadi J, Gerber BL, Coche E, Melchior J, Jashari R, Glineur D, Noirhomme P, Rubay J, El Khoury G, De Kerchove L. Stentless xenografts as an alternative to pulmonary homografts in the Ross operation. *Eur J Cardiothorac Surg*. 2013;44:e32–e39. doi: 10.1093/ejcts/ezt147.
87. Dohmen PM, Hotz H, Lembcke A, Kivelitz D, Hamm B, Konertz W. Magnetic resonance imaging of stentless xenografts for reconstruction of right ventricular outflow tract. *Semin Thorac Cardiovasc Surg*. 2001;13(4 suppl 1):24–27.
88. Habets J, Meijer TS, Meijer RC, Mali WP, Vonken EJ, Budde RP. CT attenuation measurements are valuable to discriminate pledgets used in prosthetic heart valve implantation from paravalvular leakage. *Br J Radiol*. 2012;85:e616–e621. doi: 10.1259/bjr/29602784.
89. Deutsch HJ, Bachmann R, Sechtem U, Curtius JM, Jungehülsing M, Schicha H, Hilger HH. Regurgitant flow in cardiac valve prostheses: diagnostic value of gradient echo nuclear magnetic resonance imaging in reference to transesophageal two-dimensional color Doppler echocardiography. *J Am Coll Cardiol*. 1992;19:1500–1507.
90. Nunn GR, Bennetts J, Onikul E. Durability of hand-sewn valves in the right ventricular outlet. *J Thorac Cardiovasc Surg*. 2008;136:290–296. doi: 10.1016/j.jtcvs.2008.02.063.
91. Schreiber C, Hörer J, Vogt M, Fratz S, Kunze M, Galm C, Eicken A, Lange R. A new treatment option for pulmonary valvar insufficiency: first experiences with implantation of a self-expanding stented valve without use of cardiopulmonary bypass. *Eur J Cardiothorac Surg*. 2007;31:26–30. doi: 10.1016/j.ejcts.2006.10.018.
92. Hallbergson A, Gauvreau K, Powell AJ, Geva T. Right ventricular remodeling after pulmonary valve replacement: early gains, late losses. *Ann Thorac Surg*. 2015;99:660–666. doi: 10.1016/j.athoracsur.2014.09.015.
93. Pijuan-Domenech A, Pineda V, Castro MA, Sureda-Barbosa C, Ribera A, Cruz LM, Ferreira-Gonzalez I, Dos-Subirà L, Subirana-Domènech T, Garcia-Dorado D, Casaldàliga-Ferrer J. "Pulmonary valve replacement diminishes the presence of restrictive physiology and reduces atrial volumes": a prospective study in Tetralogy of Fallot patients. *Int J Cardiol*. 2014;177:261–265. doi: 10.1016/j.ijcard.2014.09.009.
94. Habets J, Tanis W, van Herwerden LA, van den Brink RB, Mali WP, de Mol BA, Chamuleau SA, Budde RP. Cardiac computed tomography angiography results in diagnostic and therapeutic change in prosthetic heart valve endocarditis. *Int J Cardiovasc Imaging*. 2014;30:377–387. doi: 10.1007/s10554-013-0335-2.
95. Suchá D, Symersky P, Vonken EJ, Provoost E, Chamuleau SA, Budde RP. Multidetector-row computed tomography allows accurate measurement of mechanical prosthetic heart valve leaflet closing angles compared with fluoroscopy. *J Comput Assist Tomogr*. 2014;38:451–456. doi: 10.1097/RCT.0b013e3182ab5f15.
96. Lee DH, Youn HJ, Shim SB, Lee SH, Jung JI, Jung SE, Choi YS, Park CS, Oh YS, Chung WS, Kim JH. The measurement of opening angle and orifice area of a bileaflet mechanical valve using multidetector computed tomography. *Korean Circ J*. 2009;39:157–162. doi: 10.4070/kcj.2009.39.4.157.
97. Teshima H, Hayashida N, Fukunaga S, Tayama E, Kawara T, Aoyagi S, Uchida M. Usefulness of a multidetector-row computed tomography scanner for detecting pannus formation. *Ann Thorac Surg*. 2004;77:523–526. doi: 10.1016/S0003-4975(03)01531-5.
98. Teshima H, Aoyagi S, Ueda T, Takagi K, Shojima T, Tanaka H. Evaluation of advancing the standard valve dysfunction by multidetector-row CT. *J Artif Organs*. 2014;17:162–168. doi: 10.1007/s10047-013-0751-z.